Experimental cum Computational Investigation of Schiff Base and their *cis*-MoO_2(II) Complex: [MoO_2(L)(CH_3OH)]

M.K. Parte, P. K. Vishwakarma* and R. C. Maurya
Department of P.G. Studies and Research in Chemistry and Pharmacy, Rani Durgavati Vishwavidyalaya, Jabalpur (M.P.) INDIA

Abstract

Herein, we presented the experimental cum computational investigation of 4-thiophene-carbonyl-3-methyl-1-phenyl-2-pyrazolone-5-one with isonicotinic acid hydrazide-derived Schiff base: [(4Z,N'Z)-N'-((5-hydroxy-3-methyl-1-phenyl-1H-pyrazol-4-yl)(thiophen-2-yl)methylene)isonicotinohydra-zonic acid] **H_2L** and its cis-dioxidomolybdenum(II) complex [MoO_2(L)(CH_3OH)] **C1.** The compounds were formulated by physiochemistry, spectroscopy, electrochemistry, and computational methods. Results revealed that the complex has mononuclear distorted octahedral geometry. It is also predicted by geometrical properties based on the DFT method. Moreover, the compounds showed Insilco bioactivity scores and drug-likeness through the online server. The ADME properties result in the pharmaceutical chemistry of the compounds. The biological results promise their application as medicinally relevant compounds for prospects.

Keywords: MoO_2(II), Spectroscopy, Electrochemistry and Computational Studies.

INTRODUCTION

Many cis-[MoO_2](II) complexes associated with arylhydrazone Schiff base ligands have been synthesized using the ability of this metal to form stable complexes with the ligands containing different donor atoms [1]. Furthermore, molybdenum complexes have a unique place for the growth of coordination chemistry [2]. Additionally, molybdenum(VI) complexes have also paid attention due to their applied role in chemistry as catalytic activity in several oxidation reactions [3,4]. The pyrazolone derivatives, as five-membered heterocycles of pyrazoles, belong to a class of compounds highly valued in organic synthesis. Within the azole family, they are among the most extensively studied groups of compounds. Over the years, a variety of synthesis methods and synthetic similarities have been documented, highlighting their significant importance in research and applications [5]. The pyrazoline-constructed metal complexes have been reported as having effective biological relevance and pharmacological activities [6,7]. Computer-assisted techniques have significantly advanced the study of ADMET properties and presented both an economical and a time-efficient approach [8-10]. Exclusively, admetSAR was launched in the year 2012 by Y. Tang group, the first of all it is to facilitate ADMET property assessment. The admetSAR originally provided free access to over 210000 high-quality experimental data points for nearly 96000 unique compounds, and 27 models for valuation of chemical ADMET properties. It was upgraded from time to time, thereby enhancing the

quality of predictions. Despite its success, admetSAR2.0 has several drawbacks to be improved on admetSAR3.0.

In the present work, 4-thiophene-carbonyl-3-methyl-1-phenyl-2-pyrazolone-5-one and isonicotinic acid hydrazide and its dioxidomolybdenum(VI) complex was synthesized and characterized through FT-IR, ^{1}H-NMR, UV-Visible spectral studied and conductance measurements. Moreover, the insilco bio and pharmacological activity were obtained from the title compounds.

EXPERIMENTAL WORKS

Material and Methods

Reagents and solvents used in this work were commercially available and of quality AR grade. Microanalytical and NMR spectral analyses were obtained from CDRI, Lucknow. FTIR spectroscopic results were obtained from Bruker αT FT-IR spectrophotometer using KBr pallets, Electronic absorption study was recorded with Varian Carry 5000, UV/Vis/NIR spectrophotometer, electrochemistry was monitored using TBAP as supporting electrolyte with Epsilon BASi cyclic voltameter and temperature of decomposition was pointed with an melting point device with a heating capacity up to 360/ºC at our department.

The pyrazoline derivative was synthesized as the method reported by the Maurya group [11]. The Schiff base ligand was prepared by equimolar amounts of 4-thiophene-carbonyl-3-methyl-1-phenyl-2-pyrazolone-5-one (568 mg) and isonicotinic acid hydrazide (304 mg) and constant stirring and refluxed for 4 hrs at 60℃. The resulting solution of **H_2L** precipitated and filtered washed several times with methanol and dried in a desiccator over anhydrous $CaCl_2$. The complex C**1** was prepared by the refluxing of $[MoO_2(acac)_2]$ (326 mg, 1mmol) with **H_2L**, (304 mg,) in hot methanolic solution (~10 mL). The reaction mixture was refluxed for 4 hrs. at 60℃, and the resulting mixture solution $[MoO_2(L)(CH_3OH)]$ **C1**. So the desired solution was concentrated to half of its volume and then kept at room temperature for 12 hrs. The separated crystalline solid was filtered and washed several times with methanol and dried in a desiccator over anhydrous $CaCl_2$.

The compounds were formulated as for **H_2L**Yield; 0.610 g 72%, Colour; berry red, decomposition temperature; 190 ºC, Anal. Calc. for $C_{21}H_{17}O_5N_2S$ (MW: 403.18); C, 62.52; H, 4.25; N,16.59 Found: C, 54.76; H, 4.03 N, 16.59 %. Solubility; Methanol, Ethanol, Acetonitrile, DMF, and DMSO. IR (KBr, 4000-600 cm^{-1}); ν(C=N) 1630, ν(C–O) 1378 and ν(O–H) 3435, UV/Vis (DMSO) λ_{max} nm: 255 and 320. **C1**, Yield; 71.4%, Colour; Brown, decomposition temperature; 290 ºC, Anal. Calc. for $C_{22}H_{19}O_5N_5SMo$ (MW: 561); C, 67.06; H, 3.41; N,12.47 Found: C, 41.47; H, 2.77 N, 12.27 %. Solubility; Methanol, Ethanol, Acetonitrile, DMF, and DMSO. IR (KBr, 4000-600 cm^{-1}); ν(C=N) 1618, ν(C–O) 1268 and ν_s(O=Mo=O) 917, ν_{as}(O=Mo=O) 835, cm^{-1} and (CH_3OH) 3440 cm^{-1}, UV/Vis (DMSO) λ_{max} nm: 264, 328 and 426.

RESULT AND DISCUSSION

The 4-thioenyl-3-methyl-1-phenyl-2-pyrazoline-5-one and isonicotinic acid hydrazide derived Schiff base ligand: [(4Z,N'Z)-N'-((5-hydroxy-3-methyl-1-phenyl-1H-pyrazol-4-yl)(thiophen-2-yl)methylene)isonicotinohydra-zonic acid] **H_2L** and their dioxomolybdenum(VI) complex $[MoO_2(L)(CH_3OH)]$ **C1** was synthesized. The suggested structure and composition have been validated through multiple analytical techniques. The ligand and their complex decomposition temperature were also recorded; the ligand showing the value 190˚C after the complexation increase at 260˚C gives clear information about metal-ligand binding.

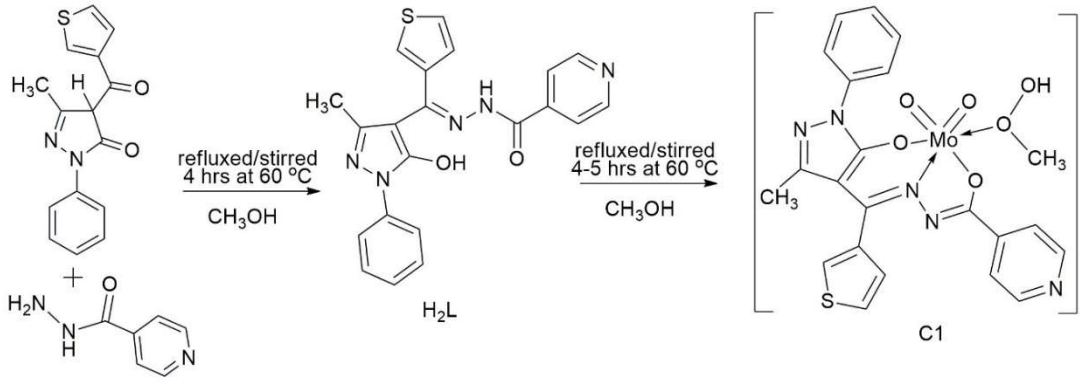

Scheme 1 Synthetic route of Schiff base ligand **H_2L** and its MoO_2(VI) complex **C1.**

Spectral Analysis

The compound observed characteristic spectral bands a broad band at 3422 cm^{-1} for ν(O-H), a sharp band at 1630 cm^{-1} due to ν(C=N), and a peak at 1662 of ν(C=O) cm^{-1}. The band of ν(N-H) is observed at 3217 cm^{-1} and is merged with the OH group. The above discussion indicates that the ligand in the present studies occurred in keto form in the solid state; after complexation, the keto form becomes an enol form due to keto-enol tautomerization. As per the structural details of the ligand, both, keto/enol tautomeric forms are demonstrated in Scheme 2. The Schiff base, a characteristic band at 1618 cm^{-1} appeared due to ν(-N=C) shifting of this band to lower wavenumbers or blue-shift in the spectrum of metal complex indicating the coordination of azomethine nitrogen to the metal center. The presence of two infrared bands in the dioxomolybdenum(VI) complex at 835 and 912 cm^{-1} asymmetric and symmetric stretching mode of cis-MoO_2 moiety [12]. The vibrational spectra of the synthesized compounds are given in Figures 1 and 2. A broad band observed at approximately ~3441 cm^{-1} is ascribed to the ν(OH) mode of coordinated methanol. This observation is further corroborated by 1H-NMR spectral analyses, which confirm the presence of coordinated methanol within the complex molecule.

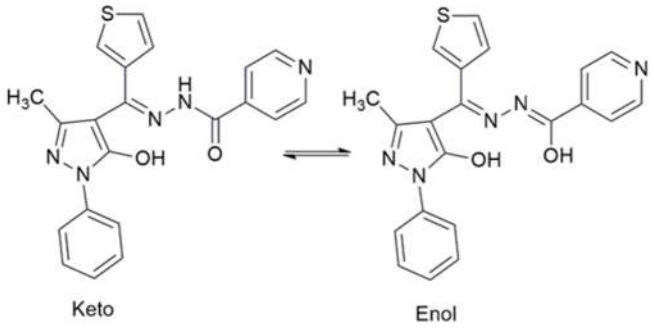

Scheme 2 Keto and enol tautomeric forms of Schiff base ligand H_2L.

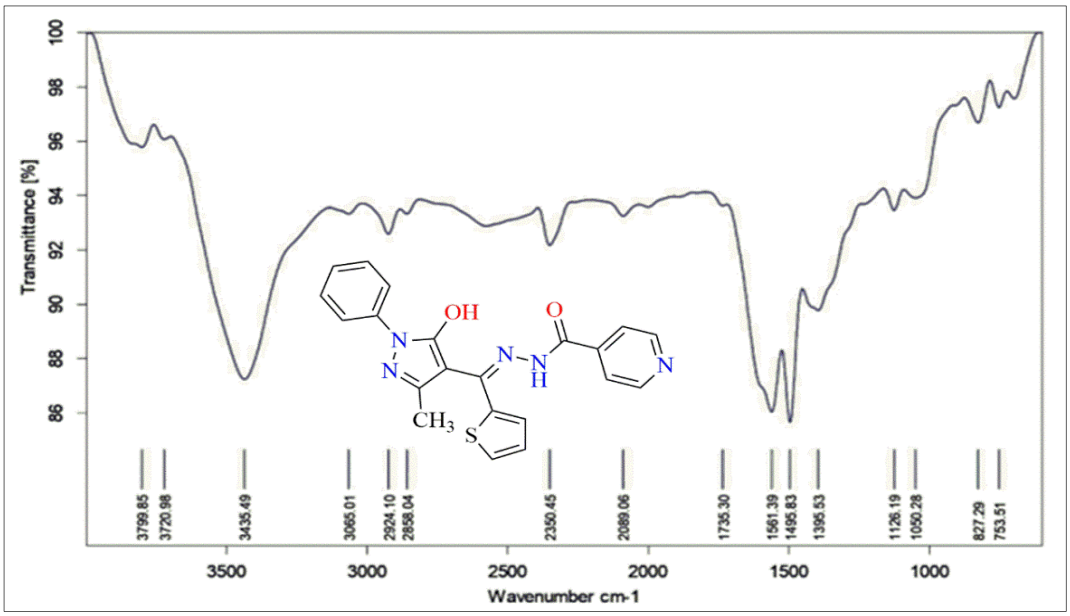

Figure 1 Experimental FT-IR spectrum of H_2L.

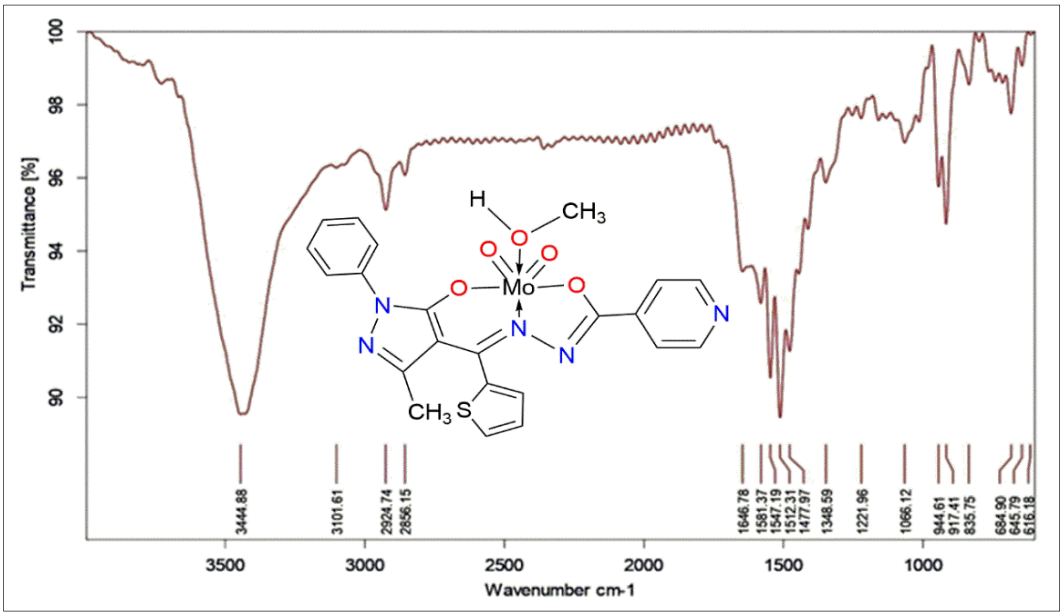

Figure 2 Experimental FT-IR spectrum of **C1**.

The electronic spectral analysis of the MoO2(II) complex was conducted in a DMSO solution, as illustrated in Figure 3. In the electronic spectral bands appear at 264 and 328 nm can be assigned to intra-ligands charge transfer (ILCT) transition n→π*/π→π* transitions. The low-intensity band at 426 nm in the visible region is most probably due to the ligand-to-metal charge transfer (LMCT) transitions. The absence of bands in the far-visible region indicates that d-d transitions do not take place in the molybdenum complexes[13].

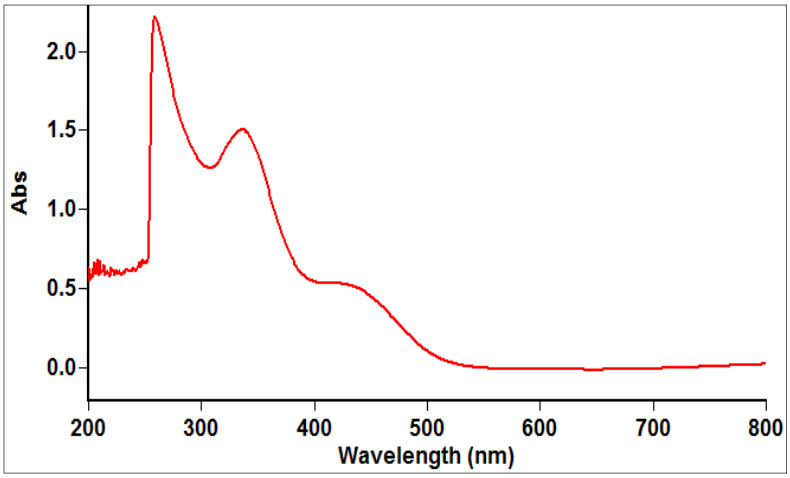

Figure 3 UV-visible spectrum of complex **C1.**

Figure 4 depicted, the ^{1}H-NMR of complex [MoO_2(L)(CH_3OH)] **C1** was recorded in DMSO-d6 at ppm**.** The complex exhibited signals at δ 8.7 ppm (s,1H, -H-C=N) due to resonance of H-C=N and hydrogen was attributed as a doublet signal, δ 7.2 (d, 1H, H-C-S) and δ 2.3 (s, 3H, H_3C-C). The signals of Aromatic-H were observed at δ 7.6–8.2 ppm. Moreover, the signal at δ = 3.32 ppm (s, 3H, H_3C-O) and δ = 3.85 ppm (s, 1H, HO-CH_3) was attributed to the proton of $HOCH_3$ group [285] of methanol it is due to coordination with the metal center.

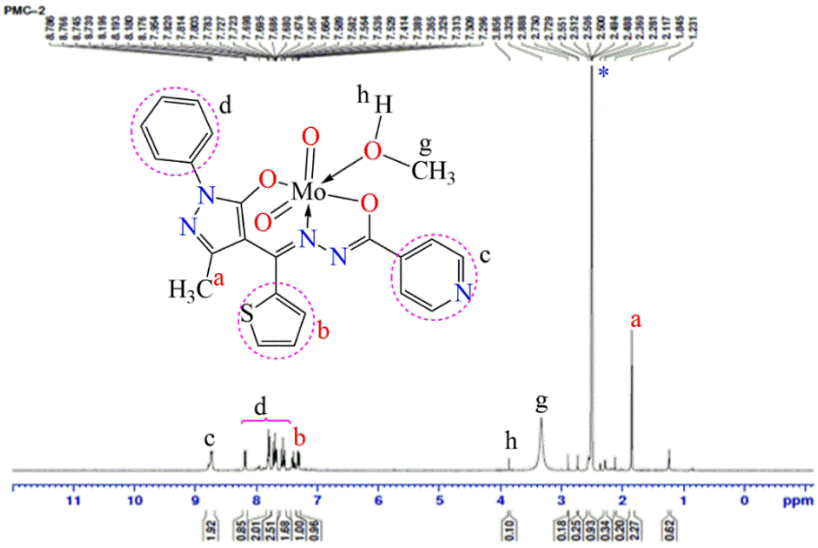

Figure 4 ^{1}H-NMR spectrum of **C1**.

Electrochemistry

The electrochemical investigation of **C1** was monitored in the potential range between ±1.500 V v/s Ag/AgCl in 0.1M solution of TBAP as an electrolyte in a mono scan range and its IUPAC mode voltammogram is presented in Figure 5. The voltammogram displayed single step irreversible reduction peak as [E_{pc}(-0.102) V], and [I_{pc} (0.268) µA] that can be used to establish as $[MoO_2]^{2+}\rightarrow[MoO_2]$ and single-step irreversible oxidation wave as [E_{pa}(-0.977) V], and [I_{pa} (0.478) µA] that can be used to establish as $[MoO_2]\rightarrow[MoO_2]^{2+}$. The corresponding formal reduction potential ($E_{1/2}$ in V) is -0.549 V. The irreversible redox property observed for the complexes may be due to the metal ion's short-lived reduced/oxidized state [14]. Electrochemical results may also be associated with FMO studies that significantly influence the formulation of chemical descriptors. The HOMO-LUMO energy and the associated separation energy Eg were determined based on the Eox(onset) potential from electrochemical measurements, as presented in Table 1. The experimental HOMO-LUMO calculation was made with the support of cyclic voltammograms, and the empirical relation for E_{HOMO} as [(E_{ox}-$E_{1/2(ferrocene)}$ +4.8] eV. The ferrocene was used as standard $E_{1/2(ferrocene)}$ is equivalent to 0.304 V, which may be used to calculate the Energy of HOMO. We can calculate Eg from the electronic absorption spectroscopy 1242/λ (nm). The value of the HOMO-LUMO and their energy gap of complex **C1** is summarized in Table 1. The molecular chemical stability is also based on the energy gap between HOMO and LUMO.

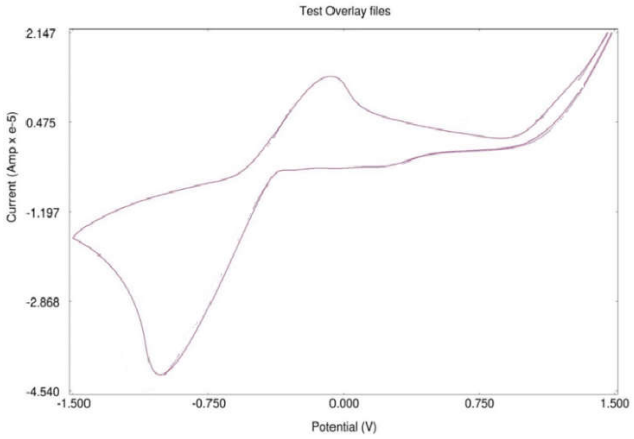

Figure 5 Cyclic voltammograms of complex C1 scan range 100 and 200 mV/Sc.

Table 1 The HOMO-LUMO values from electrochemical and electronic spectral data.

Comp.	E_{ox} V (From CV)	E_{HOMO} eV [E_{ox}-$E_{1/2}$+4.8]	Optical band gap from absorption studies (eV) 1242/λ(nm)	E_{LUMO} (E_{HOMO}- optical band gap)	$E_{HOMO-LUMO}$
C1	-0.977	3.519	4.704	-1.185	4.704

Molecular Structural Analysis

The computed molecular geometrical results of the complex compound **C1** were obtained by DFT/LANL2DZ a molecular modelling-based computational approach and their structure is depicted in Figure 6. The molecular structure of **C1** involves monomeric

molybdenum(IV) species with a cis-MoO_2^{2+} moiety. The distorted octahedral geometry consists first three coordination from a heterocyclic di-ionic tridentate ONO donor Schiff base with a basal plane and the fourth coordination from the oxygen of the MoO_2^{2+} group. The fifth and sixth coordination from the oxygen of the MoO_2^{2+} group and oxygen of coordinated methanol. Mainly the significant interatomic distance is Mo=O(31); 1.732 and Mo=O(32) 1.739 (Å). The bond angle (31)O=Mo=O(32) 106.564 (º) proves the cis-MoO_2 moiety of the studied complex. Similarly, the geometrical properties of other cis-dioxidomolybdenum(VI) complexes are reported [15,16]. Table 2, charted the selected geometrical parameters and these results suggest that the geometry of the complexes is distorted octahedral. The figure indicates the associated atoms in the molecule the oxygen atom is red, the nitrogen atom is blue the carbon is grey and the hydrogens as white colours. Figures 7 and 8 represent the bar diagram of geometrical parameters like bond length and bond angle of the selected atomic connections.

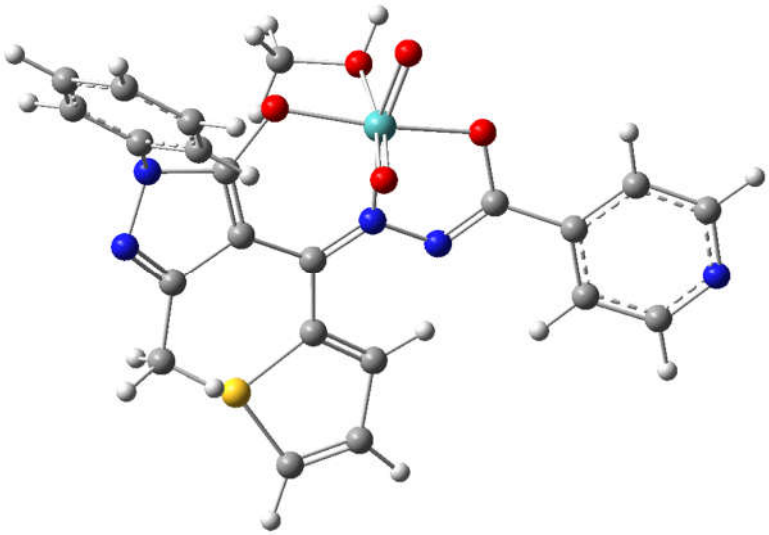

Figure 6 Computed Geometry of $[MoO_2(L)(CH_3OH)]$ **C1** was obtained by DFT/LANL2DZ.

Table 2 Selective molecular structural parameters of $[MoO_2(L)(CH_3OH)]$ C1.

Atom Connection	Inter Atomic Distance (Å)	Atom Connection	Bond Angles (°)	Atom Connection	Bond Angles (°)
Mo-O(19)	2.019	O(19)-Mo-O(27)	144.753	O(27)-Mo-O(33)	80.087
Mo-O(27)	1.981	O(19)-Mo-N(29)	80.860	N(29)-Mo-O(31)	94.006
Mo-N(29)	2.330	O(19)-Mo-O(31)	98.504	N(29)-Mo-O(32)	158.747
Mo-O(31)	1.732	O(19)-Mo-O(32)	100.824	N(29)-Mo-O(33)	77.164
Mo-O(32)	1.739	O(19)-Mo-O(33)	98.507	O(31)-Mo-O(32)	106.563
Mo-O(33)	2.417	O(27)-Mo-N(29)	60.856	O(31)-Mo-O(33)	168.434
		O(27)-Mo-O(31)	104.377	O(32)-Mo-O(33)	83.078
		O(27)-Mo-O(32)	97.881		

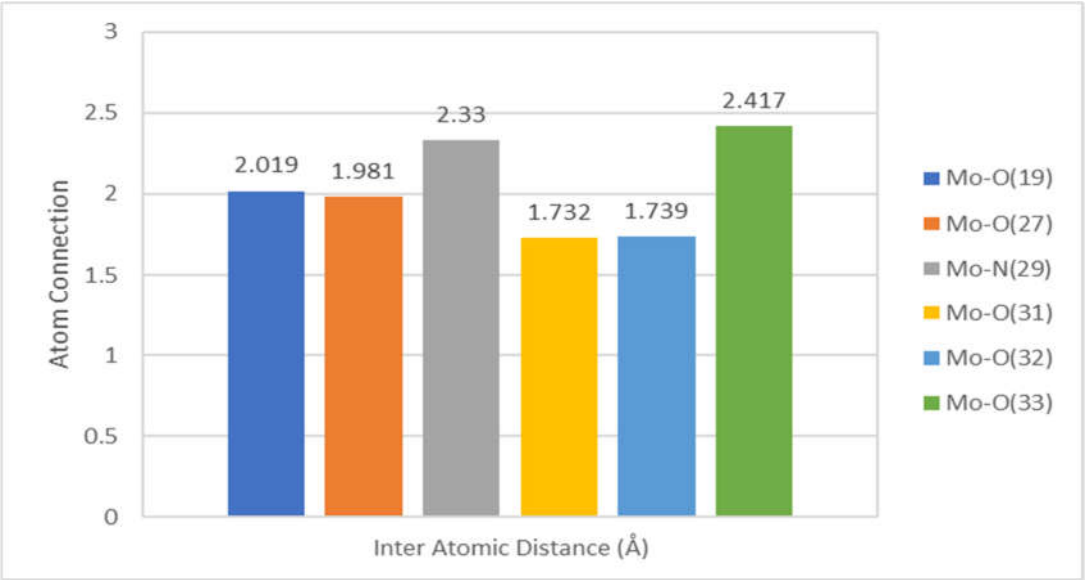

Figure 7 Plot of selected inter-atomic distance (Å) of C1**.**

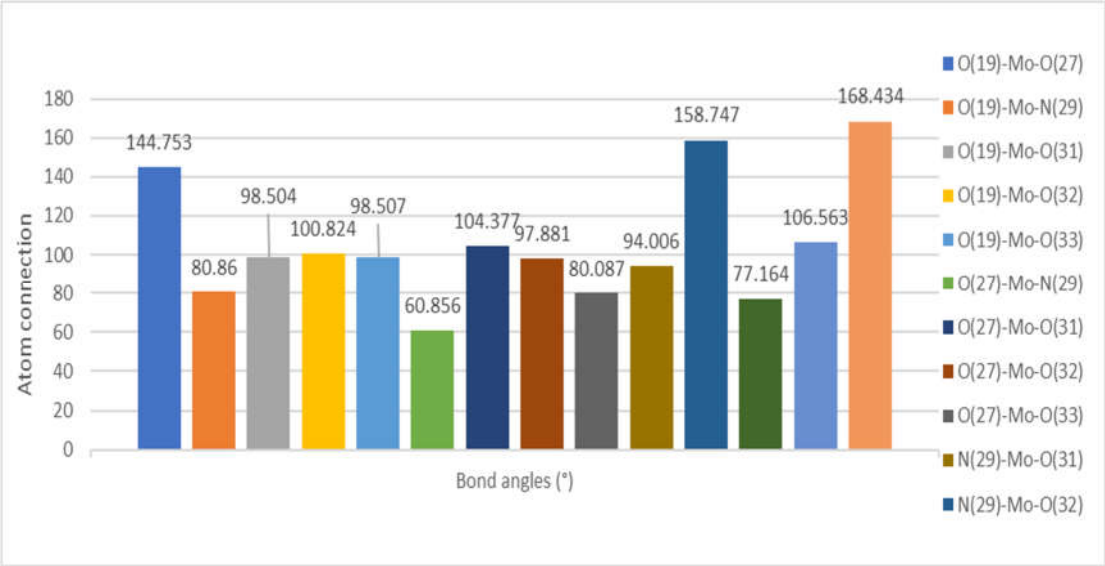

Figure 8 Plot of selected bond angles of **C1.**

Insilco Biological Prediction

The pharmacology of drugs is well-defined by their highly relevant interaction with the diversity of biological goals, including enzymes, ion channels, and receptors in living systems. The bioavailability of the title compounds was predicted by subjecting them to calculations over the web server, www.molinspiration.com, and the results are charted in Table 3. The bioactivity scores are examined based on the following five parameters:

(i) G-protein coupled receptor ligand (GPCRL)
(ii) Ion channel modulation (ICM)
(iii) Nuclear Receptor Ligand (NRL)
(iv) Protease Inhibition (PI)
(v) Enzyme Inhibition (EI)

Based on modern research outputs, substances with bioactivity scores of 0.0 or higher, the drugs are extremely bioactive, while those with scores of 5.0 to 0 have moderate activity, and those with a score of 5.0 or above are inactive [17]. The title compounds have values of -0.56 to 0.04, so they are predicted to have moderate activity [18]. These are expected to retain such properties as demand for them to behave as potential drugs with some alterations in their molecular structure [19]. A benchmark for drug design and their development by Lipinski's rule of five (RO5) assists in the description of molecular characteristics of drugs that give insight into numerous pharmacokinetic parameters, including absorption, distribution, metabolism, and excretion (ADME), for predicting the success of an orally administered drug's journey over the body to the site of action. About a certain molecular characteristic, Lipinski's rule of five (RO5) is-

(i) MlogP (partition coefficient)
(ii) Molecular weight,
(iii) Number of hydrogen bond acceptors (nON)
(iv) Hydrogen bond donors (nOHNH)
(v) Topological Polar Surface Area (TPSA)

The rule of five (RO5) predicts the oral activity of a compound. The compounds for an orally active medication should contain logP (≤5), hydrogen bond acceptors (≤10), hydrogen bond donors (≤5), and a molecular weight of (≤500), according to RO5 [20]. An orally active medicine should not typically exhibit any rule violations. Herein, the results of the title compound's % absorption, TPSA, milLogP, and other parameters are computed and charted in Table 4. Under Lipinski's Rule [21], it can be shown that the milLogP value of ligand **H_2L** is 2.38, while the complex C**1** i**s** -4.77; these are within the acceptable range for compounds as a drug to pass through bio-membranes and display good bioavailability. The title compounds meet the requirements as oral therapeutic molecules under RO5. However, the current developments in drug discovery have expanded the chemical space for candidates that are orally active drugs outside Lipinski's rule. So, the studied compounds can be considered oral therapeutic molecules as per RO5. By considering target interaction and incorporating various natural products rich in activities [22].

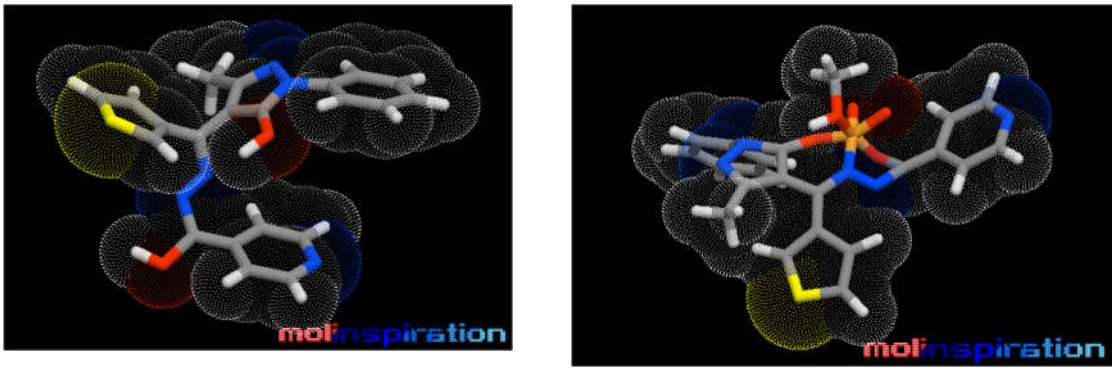

H_2L **C1**

Figure 9 3D-Molecular structures of title ligand and their metal complex obtained through Molinspiration galaxy 3D structure generator v2021.01 beta a web tool.

Table 3 Bioactivity score of the synthesized ligand and their complex C1.

Comp.	Parameters of Bioactivity Score					
	GPCR ligand	Ion channel modulator	Kinase inhibitor	Nuclear receptor ligand	Protease inhibitor	Enzyme inhibitor
H_2L	-0.25	-0.07	-0.39	-0.56	-0.34	-0.12
C1	-0.04	-0.11	-0.09	-0.39	-0.13	-0.06

Table 4 Bioactivity score of the synthesized ligand and their complex C1.

Comp.	Lipinski's Parameters							
	% Abs.	TPSA $(Å)^2$	MlogP	nOHNH	nON	nrtb		Lipinski's violations
H_2L	75.92	95.90	2.38	2	7	5	403.47	0
C1	70.01	113.03	-4.77	1	10	4	561.43	0

Percentage absorption (% abs.) was calculated by % Abs = 109-[0.345 × TPSA], Topological polar surface area (TPSA) (defined as a sum of surfaces of polar atoms in a molecule), Logarithm of compound partition coefficient between n-octanol and water, Hydrogen bond donors (nOHNH), Hydrogen bond acceptors (nON) and Number of rotatable bonds (nrotb).

After the Insilco biological activity of the title compound one more computer-aided technique was used to predict ADME properties by ADMETSAR methodology [23] web server (http://lmmd.ecust.edu.cn/admetsar2). The method is performed to investigate whether the investigated compounds produce any toxicity after administration in the body or show any pharmacokinetic profile. This methodology is based on the molecular structure of the compounds that were characterized for the prediction of their pharmacokinetics, absorption, distribution, metabolism, and excretion (ADME) and their pharmacodynamics and toxicity, to avoid potential interactions of drugs with anti-targets causing many side effects. Here various ADME models namely-

(i) Blood-brain barrier (BBB) penetration
(ii) Aqueous solubility (LogS)
(iii) Caco-2 cell permeability,
(iv) Human Intestinal Absorption (HIA),
(v) Carcinogenetic,
(vi) LD50 dosage

The predicted ADMET data of the title compounds are charted in Table 5. The compounds show high absorption, and distribution properties indicated by the higher value of HIA, BBB, and Caco2 permeability values, and it suggests the more auspicious pharmacokinetic properties. The carcinogenic profile of compounds also displayed a non-carcinogenic nature. One of the more applied features collected from ADMETSAR is the computed median lethal dose (LD50) dosage in the rat model (acute rat toxicity) which helps in deciding the lethalness of compounds. The lower the LD50 value, the more lethal the compounds are in comparison to those with higher LD50 values. The LD50 values of the

compounds examined are typically higher than that of the drug streptomycin, which has an LD50 of 1.841 mol/kg.

Table 5 ADMET activity score of the Schiff base ligand and metal complex.

Comp.	BBB	HIA	Caco2	ROCT	Carcinogenicity	LogS	LD50 mol/kg
H_2L	0.890	0.991	0.531	Non-inhibitor	Non-carcinogens	-2.4137	2.2362
C1	0.7676	0.7239	0.5683	Non-inhibitor	Non-carcinogens	-3.3641	2.6117

CONCLUSIONS

In conclusion, we discuss the experimental cum computational investigation of the pyrazoline and isonicotinic acid involving the Schiff base and their MoO_2 complex. The molecular structure of mononuclear MoO_2(II) complex naming, $[MoO_2(L^1)(MeOH)]$ **C1** was determined by geometrical results via the DFT method. From the physiochemical spectroscopic and computational results, the complex has distorted octahedral geometry with 1:1 metal-ligand stoichiometry. Additionally, the applications of the title compounds are based on insilco bioactivity and ADME results. These results are attributed to good pharmacokinetics and biological activity. The bioactivity score is -1.10 to 0.07 for these studies' compounds**.** While TPSA values are 128.5 and 117.18 Å² of compounds **H_2L,** and **C1** respectively. The LD50 values of studied compounds are 2.236 and 2.611 mostly more than that of the commonly used drug streptomycin (LD50=1.841 mol/kg).

ACKNOWLEDGMENT

The authors express their gratitude to Professor P.K. Khare, Head of the Department, for facilitating the essential analytical resources. Additionally, the authors extend their appreciation to Prof. Rajesh Kumar Verma, Vice Chancellor of Rani Durgavati Vishwavidyalaya Jabalpur, for his motivation and support.

Conflicts of Interest

No potential conflict of interest was reported by the authors.

Funding

No funding for this work.

REFERENCE

[1] M. K. Parte, P. K. Vishwakarma, P. S. Jaget and R. C. Maurya, J. Cord. Chem. 74 (2021) 584-597.

[2] Q. Zhang, A.J. Atkin, I.J. Fairlamb, A.C. Whitwood, J.M. Lynam, Organometallics 30 (2011) 4643.

[3] A. Bezaatpour, S. Khatami, M. Amiri. RSC Adv., 6, 27452, 27452 (2016).
[4] M.R. Maurya, S. Dhaka, F. Avecilla. Polyhedron, 96, 79 (2015).
[5] K. Karrouchi, S. Radi, Y. Ramli, J. Taoufik, Y. Mabkhot, F. Al-aizari, M. Ansar, Molecules 23 (2018) 23, 134
[6] P. Devi, K. Singh, D. Makawana, Chem. Biodiversity 2023, e202300072(2-9).
[7] J.S. Casas, E.E. Castellano, J. Ellena, M.S. Garcıa-Tasende, M. Luz Perez-Paralle, A. Sanchez, A. Sanchez-Gonzalez, J. Sordo and A. Touceda A. J. Inorg. Biochem. 102 (2008) 33–45.
[8] Y. Gu, Z. Yu, Y. Wang, L. Chen, C. Lou, C. Yang, W. Li, G. Liu, Y. Tang. Nucleic Acids Research, 52, W1, (2024)s W432-W438.
[9] L.L.G. Ferreira, A.D. Andricopulo, Drug Discov. Today 24 (2019) 1157-1165.
[10] C. Jia, J. Li, G. Hao, G. Yang, Drug Discov. Today, 25 (2020) 248-258.
[11] J.M. Mir, R.C. Maurya, P.K. Vishwakarma, D.K. Rajak, N. Jain, P.S. Jaget, M. Parte R. Chaurasia, M.W. Khan and P. Bohre, J Theor Comput Sci, 3 (2016) Doi:10.4172/2376-130X.1000147
[12] R.C. Maurya, J. Chourasia, M.H. Martin, S. Roy, A.K. Sharma, P. Vishwakarma, Arabian Journal of Chemistry (2015) 8, 293-306.
[13] P.K. Vishwakarma and R.C. Maurya, J. Research in Chemistry, 4 (2023)56-68.
[14] R.N. Patel, V.L.N. Gundla, D.K. Patel, Polyhedron, 27 (2008) 1054.
[15] H. Kargar, M. Fallah-Mehrjardi, M. Ashfaq, K.S. Munawar, M. N. Tahir, Journal of Molecular Structure,1294, 2(2023)136458.
[16] S.Y. Ebrahimipour, H. Khabazadeh, J. Castro, I. Sheikhshoaie, A. Crochet, K.M. Fromm, Inorganica Chimica Acta 427(2015)52-61.
[17] A. Venturini, J. A. Gonzalez, J. Org. Chem., 67 (2002) 9089.
[18] C.J. Dhanaraj, J. Johnson, J. Photochem. Photobiol. Biol., 161 (2016) 108.
[19] T. Khan, S. Dixit, R. Ahmad, S. Raza, A. Iqbal, S. Joshi, A.R. Khan, J. Chem. Bio., (2017) 91.
[20] C.A. Lipinski, F. Lombardo, B.W. Dominy, P.J. Feeney, Adv. Drug Deliv. Rev., 46 (2001) 3.
[21] P. R. Ammal, A.R. Prasad, A. Joseph Heliyon, (2020) 10.1016/j.heliyon.2020.e05144.
[22] B.C. Doak, J. Kohlberg, J. Med. Chem., 59 (2016) 2312.
[23] F. Cheng, W. Li, Y. Zhou, J. Shen, Z. Wu, G. Liu, P. W. Lee, Y. Tang, J. Chem. Inf. Model., 52 (2012) 3099.